Acetylene Hydroformylation with $HCo(CO)_3$ as Catalyst. A Density Functional Study

Chun-Fang Huo,† Yong-Wang Li,† Matthias Beller,‡ and Haijun Jiao*,†,‡

The State Key Laboratory of Coal Conversion, Institute of Coal Chemistry, Chinese Academy of Sciences, Taiyuan 030001, People's Republic of China, and Leibniz-Institut für Organische Katalyse an der Universität Rostock e.V., Buchbinderstrasse 5-6, 18055 Rostock, Germany

Received October 1, 2003

The mechanism of acetylene hydroformylation with $HCo(CO)_3$ as active catalyst has been proposed and discussed on the basis of B3LYP density functional theory computation. It is found that the characteristic catalytic cycle is similar to that for olefin hydroformylation: (a) acetylene coordination and insertion, (b) CO coordination and insertion, and (c) H_2 coordination and oxidative addition as well as unsaturated aldehyde elimination. Acetylene hydroformylation is computed to be more favored energetically than the competitive acetylene hydrogenation, and the production of saturated aldehyde is therefore due to the subsequent hydrogenation of the initially formed α,β-unsaturated aldehyde rather than the proposed hydrogenation of acetylene prior to hydroformylation. In contrast to olefin, acetylene insertion into the Co−H bond is an irreversible process, which determines the regioselectivity of terminal alkynes. CO coordination is found to be an exergonic process, while the corresponding H_2 process is endergonic, and therefore, H_2 is not competitive with CO. On the basis of the computed free energies of activation, the rate-determining step can be one of the reactions of the acyl tricarbonyl complex ($(H_2C{=}CHCO)Co(CO)_3$) with variation of the reaction conditions.

Introduction

Since its discovery by Roelen in 1938, hydroformylation, which converts olefins and synthesis gas ($H_2 + CO$) into aldehydes, has developed into an extremely important industrial process. Therefore, extensive studies have focused on the hydroformylation of olefins,[1−7] while hydroformylation of alkynes has received relatively scant attention. In 1951, Natta and Pino[8] reported a mixture of high-boiling, unidentified products by the reaction of acetylene with synthesis gas in the presence of metallic cobalt at 120−150 °C and 200−300 atm. This reaction had a lower rate than olefin hydroformylation. Despite some efforts being made,[9−15] hydroformylation of alkynes to α,β-unsaturated aldehydes had little success until the past decade. The early investigations usually resulted in low selectivity and/or low yield of unsaturated aldehydes, primarily because the formation of the corresponding saturated aldehydes and noncarbonylated olefins could hardly be suppressed. There are two possible channels for the formation of saturated aldehydes: (a) alkyne hydrogenation prior to hydroformylation and (b) hydrogenation of the initially formed unsaturated aldehydes.

During the past decade, new progress has been made in the hydroformylation of alkynes to α,β-unsaturated aldehydes. An effective catalyst, composed of $Rh(CO)_2$(acac) and a sophisticated bis-phosphite ligand, was reported by Johnson et al.[16] in 1995, and a heterobimetallic catalyst, $PdCl_2(PCy_3)_2$ and $Co_2(CO)_8$, was reported by Ishii et al.[17] in 1997. They found that the hydroformylation of internal alkynes to α,β-unsaturated aldehydes could be accomplished with high activity and selectivity. In 1999, Van den Hoven and Alper developed a catalyst system of a zwitterionic rhodium complex and triphenyl phosphite, which is of value for the hydroformylation of enynes[18] or acetylenic thiophenes[19] to

* To whom correspondence should be addressed at the Universität Rostock e.V. E-mail: hjiao@ifok.uni-rostock.de.
† Chinese Academy of Sciences.
‡ Universität Rostock e.V.

(1) (a) Van Leeuwen, P. W. N. M.; Claver, C. *Rhodium Catalyzed Hydroformylation*; Kluwer Academic: Dordrecht, The Netherlands, 2000. (b) Falbe, J. *New Syntheses with Carbon Monoxide*; Springer-Verlag: Berlin, Heidelberg, New York, 1980. (c) Torrent, M.; Solà, M.; Frenking, G. *Chem. Rev.* **2000**, *100*, 439.
(2) Beller, M.; Cornils, B.; Frohning, C. D.; Kohlpaintner, C. W. *J. Mol. Catal. A* **1995**, *104*, 17.
(3) Parshall, G. W.; Ittel, S. D. *Homogeneous Catalysis*; Wiley-Interscience: New York, 1992.
(4) Cornils, B.; Herrmann, W. A. *Applied Homogeneous Catalysis with Organometallic Compounds*; Wiley-VCH: Weinheim, Germany, 2002; Vol. 1.
(5) Orchin, M.; Rupilius, W. *Catal. Rev.* **1972**, *6*, 85.
(6) Süss-Fink, G.; Meister, G. *Adv. Organomet. Chem.* **1993**, *35*, 41.
(7) Papadogianakis, G.; Sheldon, R. A. *New J. Chem.* **1996**, *20*, 175.
(8) Natta, G.; Pino, P. The 12th International Congress of Pure and Applied Chemistry, New York, Sept 1951.
(9) Greenfield, H.; Wotiz, J. H.; Wender, I. *J. Org. Chem.* **1957**, *22*, 542.
(10) Fell, B.; Beutler, M. *Tetrahedron Lett.* **1972**, *13*, 3455.
(11) Botteghi, C.; Salomon, Ch. *Tetrahedron Lett.* **1974**, *15*, 4285.
(12) Doyama, K.; Joh, T.; Shiohara, T.; Takahashi, S. *Bull. Chem. Soc. Jpn.* **1988**, *61*, 4353.
(13) Wuts, P. G. M.; Ritter, A. R. *J. Org. Chem.* **1989**, *54*, 5180.
(14) Campi, E. M.; Jackson, W. R.; Nilsson, Y. *Tetrahedron Lett.* **1991**, *32*, 1093.
(15) Nombel, P.; Lugan, N.; Mulla, F.; Lavigne, G. *Organometallics* **1994**, *13*, 4673.
(16) Johnson, J. R.; Cuny, G. D.; Buchwald, S. L. *Angew. Chem., Int. Ed. Engl.* **1995**, *34*, 1760.
(17) Ishii, Y.; Miyashita, K.; Kamita, K.; Hidai, M. *J. Am. Chem. Soc.* **1997**, *119*, 6448.
(18) Van den Hoven, B. G.; Alper, H. *J. Org. Chem.* **1999**, *64*, 3964.

10.1021/om034212r CCC: $27.50
Publication on Web 01/14/2004

produce α,β-unsaturated aldehydes with good yield and regioselectivity. This renewed interest for obtaining α,β-unsaturated aldehydes from alkyne hydroformylation prompts us to consider the detailed catalytic mechanism. Since cobalt carbonyl complexes are very important catalysts in hydroformylation and are still the object of detailed studies,[2] we employ $HCo(CO)_3$ and acetylene to model the alkyne hydroformylation.

To our knowledge, no theoretical investigations on the hydroformylation of alkynes have been reported so far, and some relevant information is available in the literature. The structure and bonding of transition-metal carbonyl complexes, $M(CO)_5(\eta^2\text{-HC}{\equiv}\text{CH})$ (M = Cr, Mo, W) and $M(CO)_3(\eta^2\text{-HC}{\equiv}\text{CH})$ (M = Ni, Pd, Pt), have been discussed by Frenking et al.[20] As the fundamental step in catalytic processes, such as hydrogenation, isomerization, hydroformylation, polymerization, and stoichiometric transformation of organic systems, the insertion of alkyne into a metal−hydrogen (M−H) or metal−carbon (M−C) bond has been studied both experimentally[21−23] and theoretically.[24−27] Recently, the Reppe carbonylation of acetylene on nickel carbonyl has been investigated at the DFT level of theory by De Angelis et al.[28,29] In particular, the migrative insertion of CO into $Ni{-}CH{=}CH_2$ was simulated by dynamic methods. For Co-catalyzed olefin hydroformylation, the widely accepted Heck and Breslow mechanism[30] consists of six steps: (a) olefin coordination, (b) olefin insertion, (c) CO addition, (d) CO insertion, (e) H_2 oxidative addition, and (f) aldehyde reductive elimination with catalyst regeneration. Although it is intuitive to consider alkyne to have mechanistic aspects in hydroformylation similar to those of olefins, some important differences must exist, arising from the individual characters of triple and double bonds, and various mechanistic details for alkyne hydroformylation need to be elucidated. For instance, what is the most stable alkyne complex and what is the rotation barrier of the coordinated alkyne? Is alkyne insertion reversible or irreversible? Which step is responsible for the regioselectivity of linear to branched products of terminal alkyne hydroformylation? What is the rate-determining step of the entire process? How can the saturated aldehyde be formed: i.e., via alkyne hydrogenation followed by olefin hydroformylation or via the hydrogenation of the initially formed unsaturated aldehyde?

In this work, to answer the questions raised above and gain insight into the mechanism of alkyne hydroformylation, the $HCo(CO)_3$-catalyzed acetylene hydroformylation reaction has been investigated with the B3LYP density functional method, and the competitive hydrogenation of acetylene to ethylene has also been addressed. On the basis of the discussion of each elementary step, a detailed mechanism has been proposed. The mechanistic differences of olefin and alkyne have been discussed.

Computational Details

All calculations were carried out at the B3LYP/6-311+G(d) density functional level of theory, as implemented in the Gaussian 98 program.[31] This method is found to be appropriate for cobalt carbonyl chemistry, as indicated by the excellent agreement in vibration frequencies and bond dissociation energies between theory and experiment.[32] The geometries of the intermediates and the transition states were fully optimized without any symmetry constraints, if not noted otherwise. The frequency analysis was performed at the same level to confirm the optimized structures to be ground states without imaginary frequency (NImag = 0) or transition states (TS) with one imaginary frequency (NImag = 1). Especially, the lone imaginary frequency of each transition state displayed the desired displacement orientation, and the validity of each reaction path was further examined by the intrinsic reaction coordinate (IRC) calculations. The enthalpies and the Gibbs free energies of activation and reaction were calculated under actual reaction conditions of 403.15 K and 200 atm. Considering the entropy effect, our discussions are based on the free energies (ΔG) of activation and reaction, and the corresponding enthalpies (ΔH) are provided in brackets in energy profiles for comparison. The calculated total electronic energies, ZPE values, and thermal corrections to enthalpies and Gibbs free energies are provided in the Supporting Information.

Results and Discussion

In this section, the potential energy surface of acetylene hydroformylation was fully investigated by discussing a series of reasonable structures of intermediates and transition states following the Heck and Breslow mechanism. Subsequently, the hydrogenation of acetylene to ethylene, the key competitive reaction, was studied.

(A) Acetylene Coordination. The first key step of acetylene hydroformylation is coordination and insertion. The structures of the critical points associated with this step are illustrated in Figure 1, and the free energy profile for this process is shown in Figure 2. Acetylene coordination to $HCo(CO)_3$ forms the π-complex $HCo(CO)_3(\eta^2\text{-HC}{\equiv}\text{CH})$. First, we are interested in the structure and stability of the different isomers. Due to the planar C_{2v} $HCo(CO)_3$ conformation,[32] acetylene enters the cobalt coordination sphere by the C≡C bond attacking the equatorial site. Thus, two conceivable adducts can be constructed: (i) one with the C≡C bond perpendicular to the Co−H bond and (ii) the other with the

(19) Van den Hoven, B. G.; Alper, H. *J. Org. Chem.* **1999**, *64*, 9640.
(20) Ehlers, A. W.; Dapprich, S.; Vyboishchikov, S. F.; Frenking, G. *Organometallics* **1996**, *15*, 105.
(21) Appleton, T. G.; Chisholm, M. H.; Clark, H. C. *J. Am. Chem. Soc.* **1972**, *94*, 8912.
(22) Samsel, E. G.; Norton, J. R. *J. Am. Chem. Soc.* **1984**, *106*, 5505.
(23) Boese, W. T.; Goldman, A. S. *Organometallics* **1991**, *10*, 782.
(24) Rappé, A. K. *Organometallics* **1990**, *9*, 466.
(25) Ziegler, T.; Folga, E.; Berces, A. *J. Am. Chem. Soc.* **1993**, *115*, 636.
(26) Hyla-Kryspin, I.; Niu, S.; Gleiter, R. *Organometallics* **1995**, *14*, 964.
(27) de Vaal, P.; Dedieu, A. *J. Organomet. Chem.* **1994**, *478*, 121.
(28) De Angelis, F.; Re, N.; Sgamellotti, A.; Selloni, A.; Weber, J.; Floriani, C. *Chem. Phys. Lett.* **1998**, *291*, 57.
(29) De Angelis, F.; Sgamellotti, A.; Re, N. *Organometallics* **2000**, *19*, 4104.
(30) Heck, R. F.; Breslow, D. S. *J. Am. Chem. Soc.* **1961**, *83*, 4023.
(31) Frisch, M. J.; Trucks, G. W.; Schlegel, H. B.; Scuseria, G. E.; Robb, M. A.; Cheeseman, J. R.; Zakrzewski, V. G.; Montgomery, J. A., Jr.; Stratmann, R. E.; Burant, J. C.; Dapprich, S.; Millam, J. M.; Daniels, A. D.; Kudin, K. N.; Strain, M. C.; Farkas, O.; Tomasi, J.; Barone, V.; Cossi, M.; Cammi, R.; Mennucci, B.; Pomelli, C.; Adamo, C.; Clifford, S.; Ochterski, J.; Petersson, G. A.; Ayala, P. Y.; Cui, Q.; Morokuma, K.; Malick, D. K.; Rabuck, A. D.; Raghavachari, K.; Foresman, J. B.; Cioslowski, J.; Ortiz, J. V.; Stefanov, B. B.; Liu, G.; Liashenko, A.; Piskorz, P.; Komaromi, I.; Gomperts, R.; Martin, R. L.; Fox, D. J.; Keith, T.; Al-Laham, M. A.; Peng, C. Y.; Nanayakkara, A.; Gonzalez, C.; Challacombe, M.; Gill, P. M. W.; Johnson, B. G.; Chen, W.; Wong, M. W.; Andres, J. L.; Head-Gordon, M.; Replogle, E. S.; Pople, J. A. *Gaussian 98*, revision A.1; Gaussian, Inc.: Pittsburgh, PA, 1998.
(32) Huo, C.-F.; Li, Y.-W.; Wu, G.-S.; Beller, M.; Jiao, H. *J. Phys. Chem. A* **2002**, *106*, 12161.

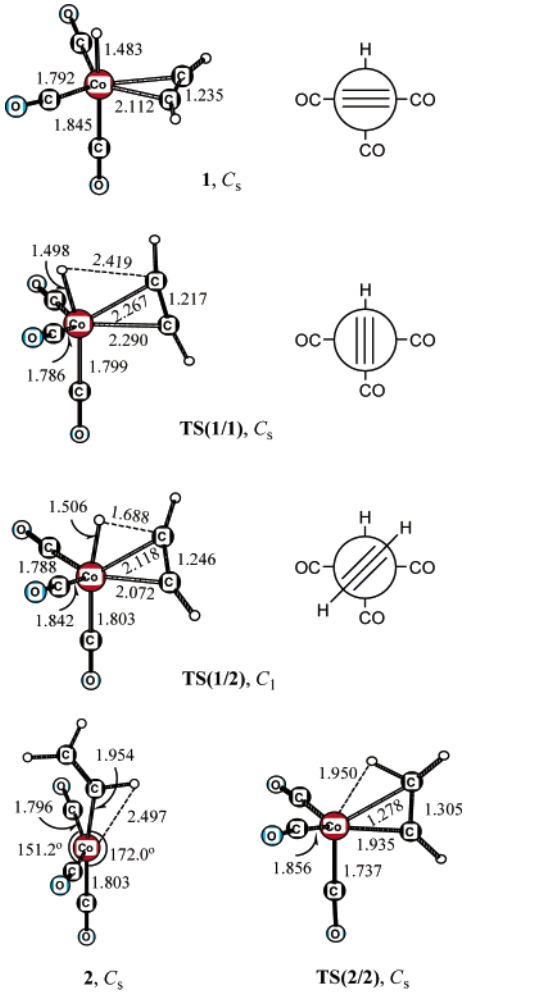

Figure 1. Bond parameters (in Å) and the Newman projection of the critical points involved in the acetylene coordination and insertion processes.

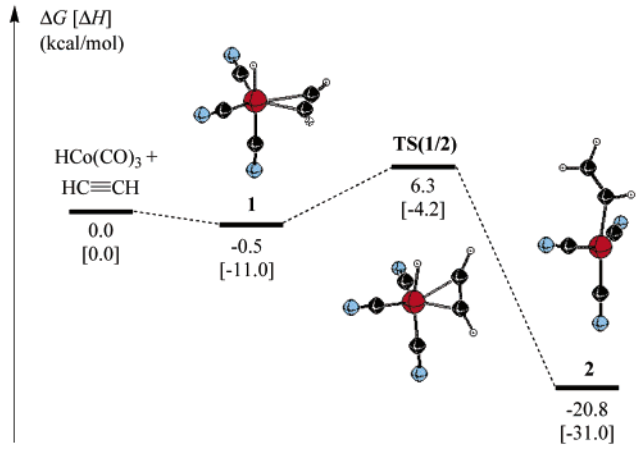

Figure 2. Free energy profile (kcal/mol, enthalpies in brackets) for the acetylene coordination and insertion (relative to $HCo(CO)_3$ + acetylene).

C≡C bond along the Co−H bond (Figure 1). It is found that conformation (i) is an energy minimum (**1**), while conformation (ii) with an imaginary frequency (39i cm^{-1}) is a transition state (**TS(1/1)**) for the acetylene rotation with a free energy barrier of 4.7 kcal/mol. This result differs from that of olefin coordination with $HCo(CO)_3$[33] and of acetylene coordination with $HNi(CO)_2Cl$,[29] in which both types of complexes are found to be the ground states.

As shown in Figure 2, acetylene coordination to $HCo(CO)_3$ forms the π-complex **1** without an energy barrier and is slightly exergonic by 0.5 kcal/mol. The bonding between acetylene and $HCo(CO)_3$ in **1** can be described by the synergic donation and back-donation model.[34] Since acetylene has two sets of mutually orthogonal π-bonds, it can bind to the cobalt fragment in double donation and back-donation fashions,[35] respectively. The hydrogen atoms of acetylene in **1** are tilted away from cobalt by 21°. The similar behavior of the ethylene complex has been ascribed to favor orbital interactions between ethylene and cobalt by raising the energy of the ethylene π-orbital and lowering the energy of the ethylene π^*-orbital.[36] This synergic effect in **1** is reflected by the elongated C≡C distance of 1.235 Å with respect to free acetylene (1.199 Å) and by the shorter Co−C distance in the acetylene complex as compared to that in the ethylene complex (2.112 vs 2.137 Å). This interaction is also evidenced by the computed vibrational frequencies. For example, the C≡C stretching frequency in **1** of 1801 cm^{-1} is lower than in free acetylene (1991 cm^{-1}), revealing the reduced triple-bond character.

(B) Acetylene Insertion. The free energy profile in Figure 2 clearly shows that the insertion of acetylene into the Co−H bond leads to the unsaturated vinyl complex $(H_2C{=}CH)Co(CO)_3$ (**2**), which has a butterfly geometry with the vinyl group in the axial site. It should be noted that the distance of 2.497 Å between Co and H(α) in **2** is much longer than the agostic interacted distances in propyl or isopropyl complexes (1.811 and 1.804 Å).[33] Thus, there is no agostic interaction in **2**. For comparison, we optimized a C_s form with the vinyl group at the equatorial position and a Co···H agostic interaction at the axial position (1.950 Å, Figure 1) and found that this structure has an imaginary frequency (301i cm^{-1}) as a transition state (**TS(2/2)**) for the degenerate rotation between two equivalent forms of **2**. With respect to **2**, **TS(2/2)** is 19.2 kcal/mol higher in free energy.

According to the above discussion on the conformations of **1** and **TS(1/1)**, one can imagine that the transition state for the acetylene insertion should have a conformation between these two limited cases. As shown in Figure 1, we located a transition state **TS(1/2)** with an imaginary mode (653i cm^{-1}) indicating Co−H insertion into the C≡C triple bond. On the basis of the Newman projection, the acetylene unit in **TS(1/2)** is rotated, and the torsion angle between the acetylene unit and the Co−H bond is −25.7°. As compared with **1**, the Co−H and C≡C bonds become longer (1.506/1.246 vs 1.483/1.235 Å), while the Co−C≡ distances become shorter (2.072/2.118 vs 2.112 Å). The most significant change in **TS(1/2)** is the shorter distance between the migrating hydrogen atom and the acetylene carbon atom (1.688 Å).

(33) Huo, C.-F.; Li, Y.-W.; Beller, M.; Jiao, H. *Organometallics* **2003**, *22*, 4665.
(34) (a) Dewar, M. J. S. *Bull. Soc. Chim. Fr.* **1951**, *18*, C71. (b) Chatt, J.; Duncanson, L. A. *J. Chem. Soc.* **1953**, 2939.
(35) Tatsumi, K.; Hoffmann, R.; Templeton, J. L. *Inorg. Chem.* **1982**, *21*, 466.
(36) Versluis, L.; Ziegler, T.; Fan, L. *Inorg. Chem.* **1990**, *29*, 4530.

From the corresponding free energy profile in Figure 2, we can see that the acetylene insertion is a one-step process with a free energy barrier of 6.8 kcal/mol. However, analysis following the imaginary mode shows a coupled process of the Co−H insertion and the skeletal Berry pseudorotation, similar to the ethylene insertion of $Rh(H)(C_2H_4)(CO)_2(PH_3)$.[37] Furthermore, the acetylene insertion reaction is predicted to be exergonic by 20.3 kcal/mol and, thus, is an irreversible process (the barrier for the back reaction is 27.1 kcal/mol). As a consequence, no isomerization of internal to terminal alkynes can be expected. Therefore, the regioselectivity of linear to branched products for utilizing terminal alkynes other than acetylene as substrates should be controlled by the irreversible insertion step. This thermodynamic behavior of the acetylene insertion into the Co−H bond differs strongly from that of olefins with $HCo(CO)_3$ as catalyst, since the latter process is reversible and thermally neutral and shows the ability of the transformation of internal to terminal olefins.[33] That the proposed regioselectivity of $HCo(CO)_3$-catalyzed acetylene hydroformylation is due to an irreversible insertion process is in agreement with olefin hydroformylation using modified Rh catalysts.[38]

(C) CO Addition and Insertion. Once the coordinatively unsaturated vinyl species **2** is formed, the CO can attach to it, and then the carbonylation reaction occurs (the competitive H_2 coordination leading to acetylene hydrogenation is discussed later). The structures of the corresponding critical points are depicted in Figure 3, whereas the free energy profile for this process is reported in Figure 4.

CO addition to **2** forms the intermediate $(H_2C{=}CH)Co(CO)_4$ (**3**). On the basis of the butterfly conformation of **2**, the incoming CO can attack the equatorially free coordination position. As illustrated in Figure 3, the most stable structure (**3**) has a conformation in which the α-hydrogen of the vinyl group is eclipsed with one of the equatorial carbonyl groups. In addition to **3**, we are interested in the additional transition state. However, all attempts to locate a transition state connecting **2** and **3** failed, and the addition reaction takes place without any barrier and is highly exergonic by 8.1 kcal/mol, as shown in Figure 4. This is in contrast to the CO addition to propyl or isopropyl complexes with small activation energies (3.7 and 4.6 kcal/mol, respectively).[33] This contrasting behavior can be ascribed to the absence of the agostic interaction in **2**.

The subsequent step is the CO insertion or carbonylation in $(H_2C{=}CH)Co(CO)_4$ (**3**). The CO insertion is a migration of the vinyl group from cobalt to the carbon atom of one of the equatorial CO ligands. The approaching Co−C distance in **TS(3/4a)** becomes shorter than in **3** (1.761 vs 1.832 Å), and **TS(3/4a)** has a strongly distorted trigonal bipyramidal conformation in which the vinyl group is at the equatorial position and the inserting CO at the axial position. In **TS(3/4a)**, $Co-C_{vinyl}-C_{carbonyl}$ forms a three-membered ring, in which the breaking Co−C bond is elongated to 2.098 Å and the forming $C_{vinyl}-C_{carbonyl}$ bond is 1.867 Å. In addition, the imaginary vibrational mode (232i cm^{-1}) indicates

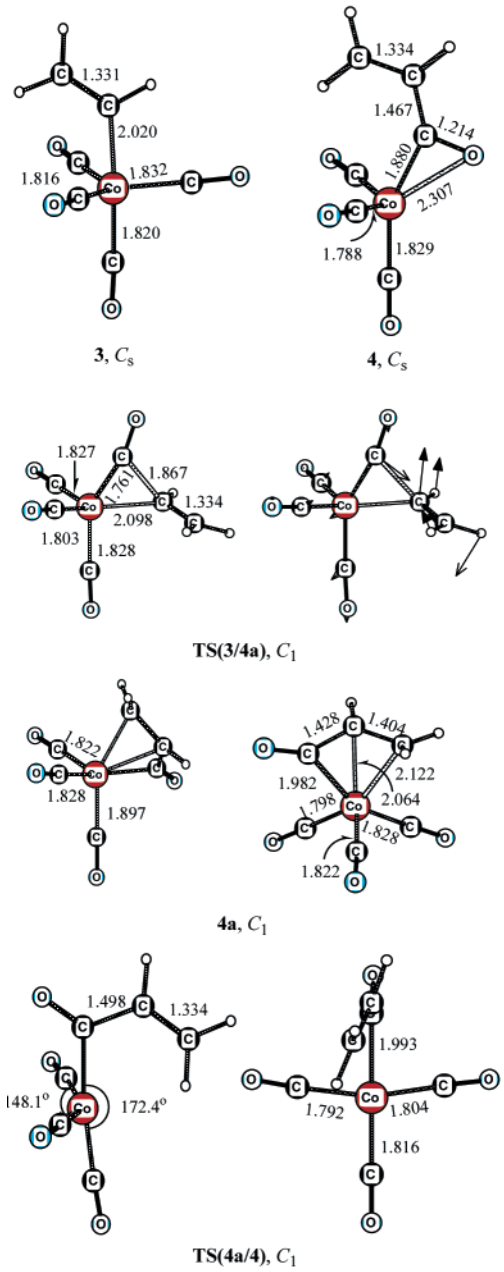

Figure 3. Bond parameters (in Å) of the critical points involved in the carbonylation process.

the coming together of the vinyl α-carbon and the carbon of the equatorial CO ligand. Following the imaginary mode directing to the insertion product, we have located a minimum structure (**4a**) with η^3 coordination between the $Co(CO)_3$ unit and the H_2CCHCO group in a square-pyramidal conformation (or distorted trigonal bipyramid, depending on the orientation). Further rotation of the $H_2C{=}CH-CO$ group around the $Co-C_{acyl}$ bond forms **4**, which has the acyl group in the axial site and is stabilized by the acyl oxygen adopting η^2-O=C coordination in the vacant equatorial site (Figure 3).

As shown in Figure 4, the carbonylation of vinyl complex **3**, forming the η^3-acyl complex **4a**, is exergonic by 1.8 kcal/mol with a free energy barrier of 8.0 kcal/mol. Isomer **4** is 3.2 kcal/mol less stable than **4a**, and this transformation process requires overcoming a free energy barrier of 11.8 kcal/mol. The present work reveals that the detailed pathway for the vinyl complex

(37) Koga, N.; Jin, S. Q.; Morokuma, K. *J. Am. Chem. Soc.* **1988**, *110*, 3417.
(38) Casey, C. P.; Petrovich, L. M. *J. Am. Chem. Soc.* **1995**, *117*, 6007.

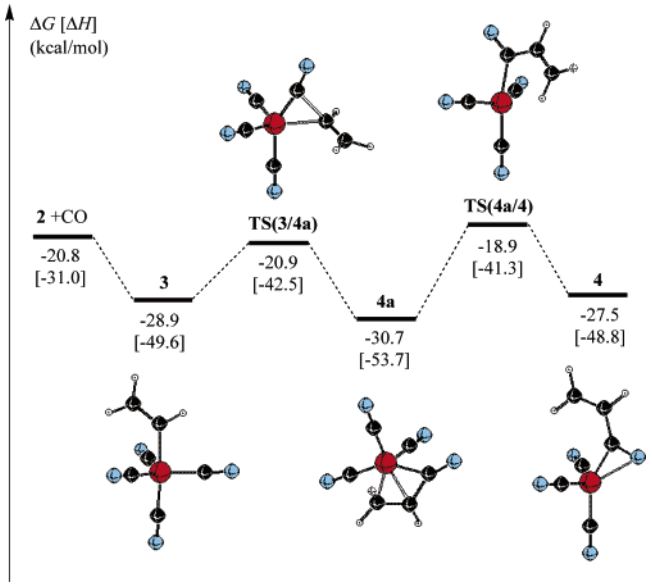

Figure 4. Free energy profile (kcal/mol, enthalpies in brackets) for the CO addition and insertion (relative to $HCo(CO)_3$ + acetylene + CO).

carbonylation differs from the recent results for the alkyl species $RCo(CO)_4$ (R = CH_3,[39] C_3H_7[33]). It was found that the CO insertion from $RCo(CO)_4$ to the η^2-acyl complex $(RCO)Co(CO)_3$ goes via two pseudorotated transition states and a Co···H−C stabilized intermediate.

(D) H_2 Oxidative Addition. Since there are two stable intermediates close in energy (**4** and **4a**), one might ask whether the subsequent hydrogenation processes leading to product occurs on **4** or **4a**. Both possibilities are considered. The optimized structures of the various critical points are shown in Figure 5, and the corresponding energy profile is represented on the left side of Figure 6.

First, we consider the more stable η^3-acyl complex **4a**. As shown in Figure 6, H_2 addition to **4a** directly leads to the complex $HCo(CO)_3(CH_2{=}CHCHO)$ (**6′**), in which acrolein coordinates with $HCo(CO)_3$ through the C=C bond. This process is slightly exergonic by 1.7 kcal/mol but has a larger free energy barrier of 37.9 kcal/mol (via **TS(4a/6′)**). As shown in Figure 5, H_2 coordination is coupled with the dissociation of the H−H bond; one hydrogen atom attacks the cobalt center to form the Co−H bond, and the other attacks the acyl carbon atom to form the CHO group. In **TS(4a/6′)**, the $Co-C_{acyl}$ bond is broken, and the H−H bond length is elongated to 0.862 Å (0.742 Å in free H_2). Thermodynamically, H_2 addition to the η^3-acyl complex **4a** can be accessible, but the high activation barrier hinders this alternative pathway.

Next, we direct our attention to the η^2-acyl complex **4**. The H_2 coordination to **4** forms the dihydrogen complex $(H_2C{=}CHCO)Co(CO)_3(\eta^2\text{-}H_2)$ (**5a**). For the corresponding transition state **TS(4/5a)**, the imaginary frequency (230i cm^{-1}) displays the approach of H_2 to the cobalt fragment. As shown in Figure 5, the attacking H_2 occupies the unsaturated equatorial site of the Co center in a side-on orientation (η^2-H_2) due to the proper orbital interaction and the simultaneous break of the

(39) Goh, S. K.; Marynick, D. S. *Organometallics* **2002**, *21*, 2262.

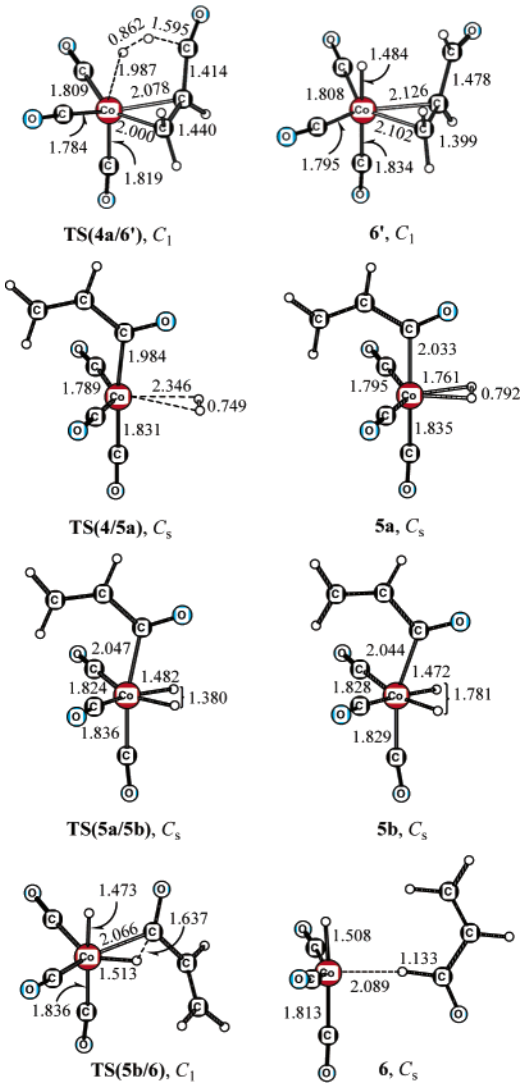

Figure 5. Bond parameters (in Å) of the critical points involved in the H_2 oxidative addition and the unsaturated aldehyde elimination processes.

η^2-O=C interaction. In **TS(4/5a)**, the H−H distance is slightly elongated with respect to that of free H_2 (0.749 vs 0.742 Å). Interestingly, H_2 coordination to the η^2-acyl complex **4** leads to the dihydrogen complex **5a** by overcoming a moderate free energy barrier of 10.7 kcal/mol. Furthermore, this coordination process is endergonic by 12.7 kcal/mol.

As depicted in Figure 5, the dihydride complex **5b**, the oxidative addition product, has a slightly distorted octahedral geometry. As compared to **5a**, the H−H distance in **5b** becomes longer and the Co−H bonds become shorter. Along with the opening of the H−Co−H angle from 26.0° (**5a**) to 74.5° (**5b**), the bond angle between two equatorial carbonyl ligands decreases from 134.4 to 110.9°. Furthermore, we found the transition state **TS(5a/5b)**, which has an imaginary frequency (577i cm^{-1}) and connects the dihydrogen complex **5a** and dihydride complex **5b** directly. The H−H distance of 1.380 Å in **TS(5a/5b)** is longer than that in **5a** (0.792 Å) but shorter than that in **5b** (1.781 Å). The Co−H bond lengths decrease from **5a** (1.761 Å) to **TS(5a/5b)** (1.482 Å) and to **5b** (1.472 Å), respectively. The energy profile in Figure 6 demonstrates that this H_2 oxidative addition

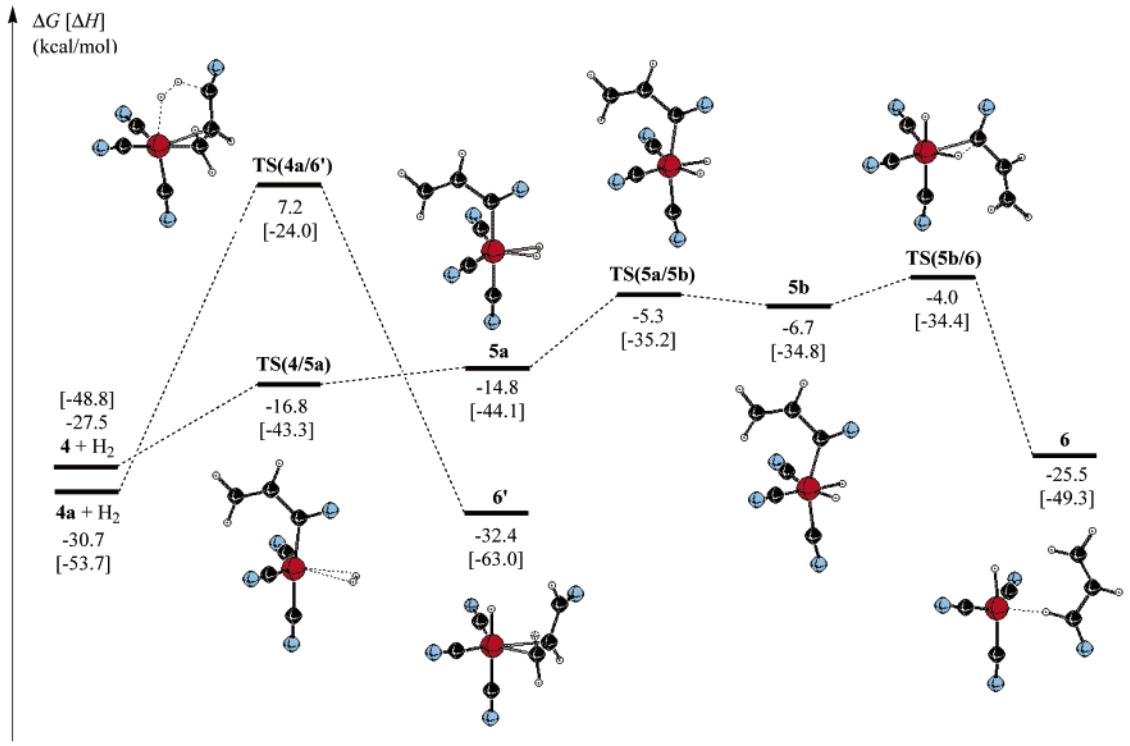

Figure 6. Free energy profile (kcal/mol, enthalpies in brackets) for the H_2 oxidative addition and the unsaturated aldehyde elimination (relative to $HCo(CO)_3$ + acetylene + CO + H_2).

process is endergonic by 8.1 kcal/mol with a free energy barrier of 9.5 kcal/mol.

(E) Reductive Elimination with the Formation of Aldehyde and Catalyst Regeneration. Following the H_2 oxidative addition, the elimination reaction occurs, and the unsaturated aldehyde product is formed. The optimized structures are illustrated in Figure 5, and the energetic data are reported on the right side of Figure 6. The elimination of acrolein from complex **5b** gives the adduct **6**, in which acrolein coordinates with $HCo(CO)_3$ through the aldehyde hydrogen atom. In addition, the elimination process goes via the three-centered transition state **TS(5b/6)** by the hydride ligand migrating and attacking the acyl carbon atom. Similar to the case for **5b**, **TS(5b/6)** also has a distorted-octahedral conformation, and the difference is that the acyl group is at the axial position in **5b**, but at the equatorial in **TS(5b/6)**. The net effect is an exchange of ligands from axial to equatorial positions. In **TS(5b/6)**, the distance between the migrating hydrogen atom and the acyl carbon atom is 1.637 Å, while the Co−C_{acyl} and Co−H bonds are still rather short. From the free energy profile in Figure 6, it is evident that the acrolein elimination is a highly exergonic (−18.8 kcal/mol) and irreversible process with a free energy barrier of 2.7 kcal/mol.

(F) CO Addition to η^2-Acyl Species: An Important Competitive Side Reaction. In addition to the H_2 coordination to η^2-acyl complex **4**, the related CO coordination is a potential competitive side reaction. The optimized structures and relative energies of the intermediate and transition state are shown in Figure 7. The incoming CO can attack the vacant equatorial site of **4**, accompanied by the breaking of the η^2-O═C interaction to form complex **5c**, $(H_2C{=}CHCO)Co(CO)_4$. In the transition state **TS(4/5c)**, the distance between the

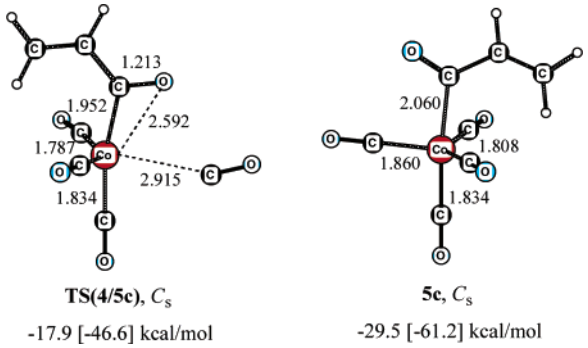

Figure 7. Bond parameters (in Å) and relative free energies (relative to $HCo(CO)_3$ + acetylene + 2CO, enthalpies in brackets) for the CO addition to acyl species $(C_2H_3CO)Co(CO)_3$ (**4**).

incoming CO and the cobalt is much longer than that in **5c** (2.915 vs 1.860 Å). The rather long acyl C═O bond (1.213 Å) and the relatively short Co−O distance (2.592 Å) indicate that there still is a weak η^2-O═C interaction in the transition state. In contrast to H_2 coordination, CO coordination is exergonic by 2.0 kcal/mol, with a free energy barrier of 9.6 kcal/mol. It is interesting to analyze the competition between H_2 and CO coordination to the η^2-acyl complex **4**. One can consider an equilibrated substitution reaction connecting **5a** and **5c** in eq 1. The large endergonic value of 14.7 kcal/mol

$$\underset{\mathbf{5c}}{(H_2C{=}CHCO)Co(CO)_4} + H_2 = \underset{\mathbf{5a}}{(H_2C{=}CHCO)Co(CO)_3(\eta^2\text{-}H_2)} + CO \quad (1)$$

$$\Delta G = 14.7 \text{ kcal/mol}$$

indicates that H_2 addition is not competitive under the

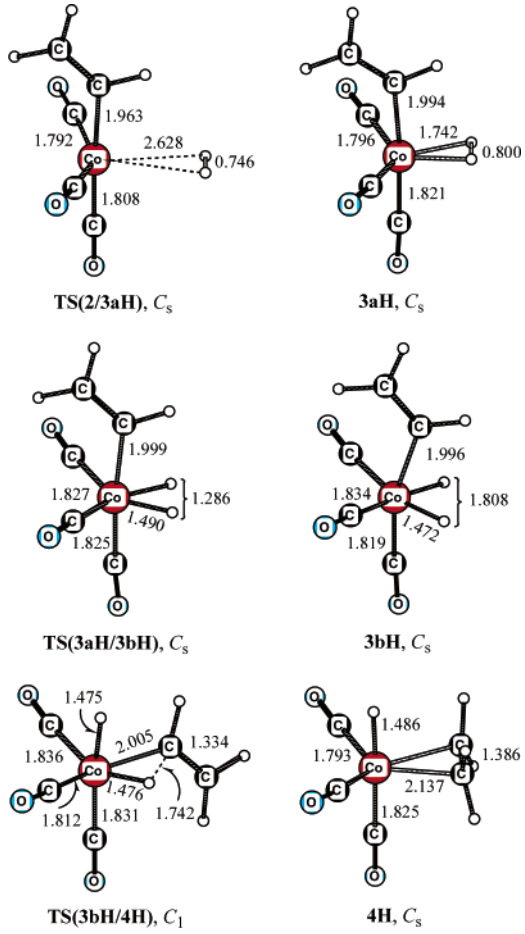

Figure 8. Bond parameters (in Å) of the critical points involved in the hydrogenation of the vinyl complex (H_2C=CH)$Co(CO)_3$ (**2**).

stoichiometric conditions. Therefore, optimization of H_2 concentration or partial pressure is essential for the reaction rate.

(G) Acetylene Hydrogenation: A Possible Competition. As mentioned in the Introduction, the formation of saturated aldehyde via the acetylene hydrogenation and olefin hydroformylation route may be a potential competitive reaction to produce unsaturated aldehyde. In this section, we explore the detailed reaction path of acetylene hydrogenation. The optimized structures are illustrated in Figure 8, and the energetic data are given in Figure 9.

During the acetylene insertion step, the vinyl complex (H_2C=CH)$Co(CO)_3$ (**2**) is formed. Like CO, H_2 can also occupy the vacant site of **2** for the hydrogenation reaction. The first step is H_2 coordination to **2** leading to the dihydrogen complex (H_2C=CH)$Co(CO)_3(\eta^2$-$H_2)$ (**3aH**). The related transition state **TS(2/3aH)** is structurally very similar to **2** and free H_2. Moreover, H_2 coordination to the vinyl complex **2** is endergonic by 7.6 kcal/mol, with a free energy barrier of 5.0 kcal/mol. In comparison with the corresponding course of H_2 coordination to acyl complex **4** (endergonic by 12.7 kcal/mol), H_2 coordination to the vinyl complex **2** is less endergonic. This is in line with the experimental finding for the relevant species $CH_3Co(CO)_3$ and $(CH_3CO)Co(CO)_3$.[40,41] Following the H_2 coordination, the oxidative addition reaction occurs. For this step, we found the transition state **TS(3aH/3bH)** connecting the dihydrogen complex **3aH** and dihydride complex **3bH** directly. As shown in Figure 8, this oxidative addition path **3aH** → **TS(3aH/3bH)** → **3bH** is very similar to that of the corresponding acyl species (**5a** → **TS(5a/5b)** → **5b**) from a structural point of view. Furthermore, the free energy profile in Figure 9 demonstrates that this oxidative addition process is endergonic by 6.2 kcal/mol, with a free energy barrier of 7.0 kcal/mol.

The subsequent step is the formation of the ethylene complex **4H** from the dihydride complex **3bH**. It is found that this process proceeds via the three-centered transition state **TS(3bH/4H)**, leading to the most stable ethylene π-complex **4H**, $HCo(CO)_3(\eta^2$-H_2C=$CH_2)$, in which ethylene coordinates to $HCo(CO)_3$ with the C=C bond in the equatorial plane. As depicted in the corresponding free energy profile in Figure 9, this process is

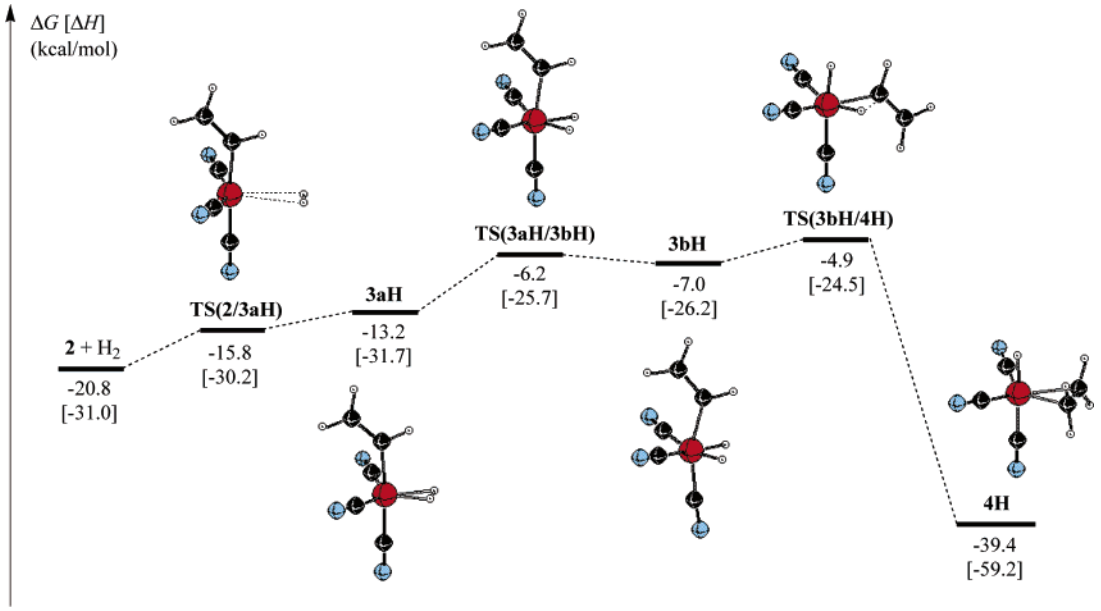

Figure 9. Free energy profile (kcal/mol, enthalpies in brackets) for the hydrogenation of the vinyl complex (H_2C=CH)-$Co(CO)_3$ (**2**) (relative to $HCo(CO)_3$ + acetylene + H_2).

Scheme 1. Free Energy Profiles (in kcal/mol) for Acetylene Hydroformylation (Dotted Lines) and Hydrogenation (Solid Lines)

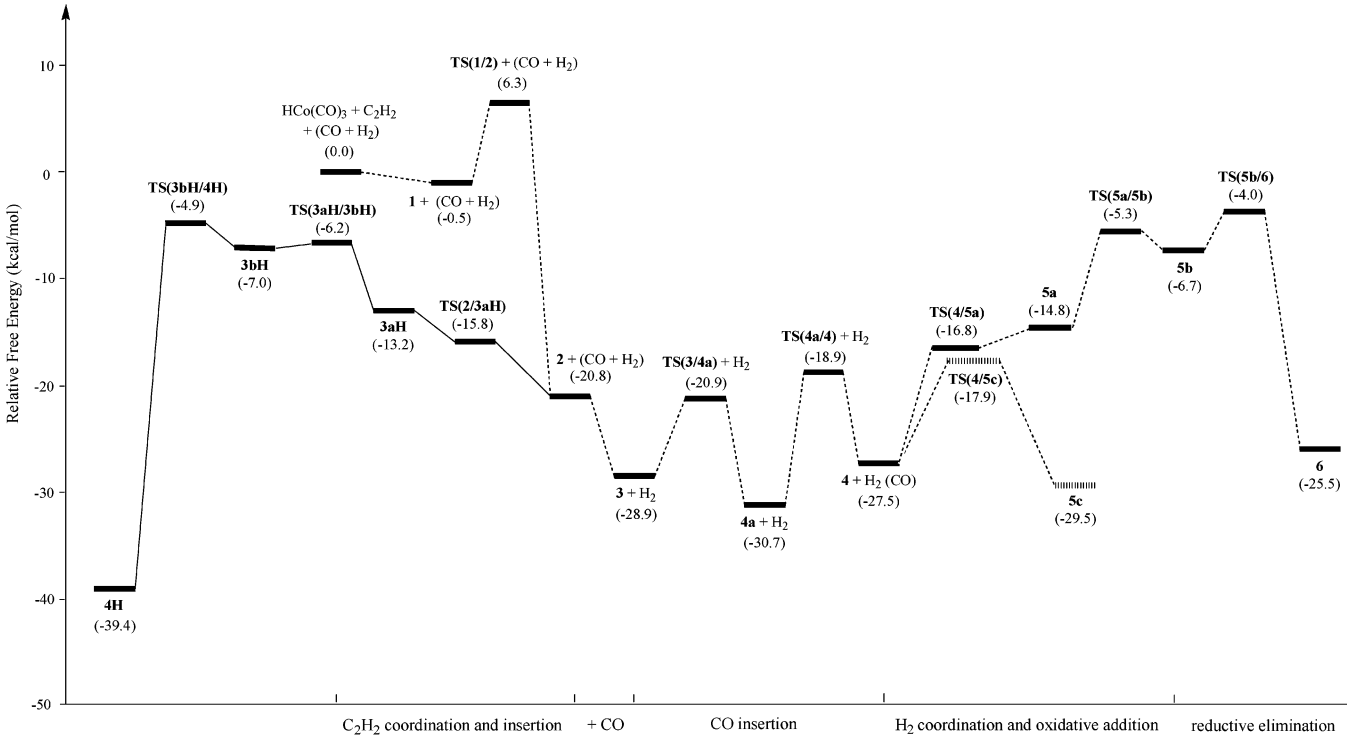

highly exergonic (−32.4 kcal/mol) and irreversible, with a small free energy barrier of 2.1 kcal/mol. As in the case of the competitive substitution between **5c** and **5a**, one can use the same principle to analyze the possible equilibrium between **3** and **3aH** in eq 2. The endergonic

$$\underset{\mathbf{3}}{(H_2C{=}CH)Co(CO)_4} + H_2 = \underset{\mathbf{3aH}}{(H_2C{=}CH)Co(CO)_3(\eta^2\text{-}H_2)} + CO \quad (2)$$

$$\Delta G = 15.7 \text{ kcal/mol}$$

property (15.7 kcal/mol) indicates that H_2 addition is not competitive with CO addition. These results reveal that acetylene hydroformylation is a more favored reaction path than acetylene hydrogenation, and therefore, the formation of saturated aldehyde is due to the further hydrogenation of the unsaturated aldehyde from hydroformylation.

Summary and Conclusion

Summarizing the results of each individual step discussed above, the complete free energy surface for the acetylene hydroformylation employing the active catalyst species $HCo(CO)_3$ is constructed in Scheme 1, and the detailed mechanism is depicted in Scheme 2. The mechanism reveals that acetylene hydroformylation for producing unsaturated aldehyde takes place along a pathway similar to that for the olefins: (i) acetylene coordination and insertion, (ii) CO addition and insertion, and (iii) H_2 coordination and oxidative addition as well as unsaturated aldehyde elimination with catalyst regeneration.

The acetylene coordination to the active catalyst $HCo(CO)_3$ forms the most stable π-complex, $HCo(CO)_3(\eta^2\text{-}HC{\equiv}CH)$ (**1**), with the C≡C bond in the equatorial plane. The following step of acetylene insertion into the Co−H bond proceeds via a square-pyramidal transition state, leading to the stable vinyl complex $(H_2C{=}CH)Co(CO)_3$ (**2**), which has a butterfly geometry with a vinyl group in the axial site. In addition, acetylene insertion is an exergonic (−20.3 kcal/mol) and irreversible process (Scheme 2), in contrast to the thermal neutral process of olefins. Therefore, one can expect that the regioselectivity of terminal alkynes RC≡CH with $HCo(CO)_3$ leading to linear and branched products should be controlled by this irreversible insertion step. It should be noted that the regioselectivity of olefin hydroformylation with a modified Rh catalyst is determined by the irreversible olefin insertion step found experimentally.

The subsequent CO addition to **2** leads to the formation of the vinyl tetracarbonyl cobalt complex $(H_2C{=}CH)Co(CO)_4$ (**3**), and the possible competitive side reaction is the formation of the dihydrogen complex $(H_2C{=}CH)Co(CO)_3(\eta^2\text{-}H_2)$ (**3aH**). The CO coordination does not have any barrier and is exergonic by 8.1 kcal/mol, while H_2 coordination is endergonic by 7.6 kcal/mol. An equilibrated CO and H_2 exchange (eq 2) indicates that H_2 coordination is not competitive thermodynamically. This rules out the possibility of acetylene hydrogenation prior to hydroformylation for the formation of saturated aldehydes under the stoichiometric conditions, and saturated aldehydes should be produced from the hydrogenation of the initially formed α,β-unsaturated aldehydes. The energetic data in Scheme 1 show that acetylene hydrogenation is in general a higher energetic process than hydroformylation, but the

(40) Sweany, R. L.; Russell, F. N. *Organometallics* **1988**, *7*, 719.
(41) Sweany, R. L. *Organometallics* **1989**, *8*, 175.

Scheme 2. Mechanism of Acetylene Hydroformylation and Hydrogenation Catalyzed by $HCo(CO)_3$ on the Basis of the Free Energies (kcal/mol) of Activation and Reaction at the B3LYP/6-311+G(d) Level of Theory

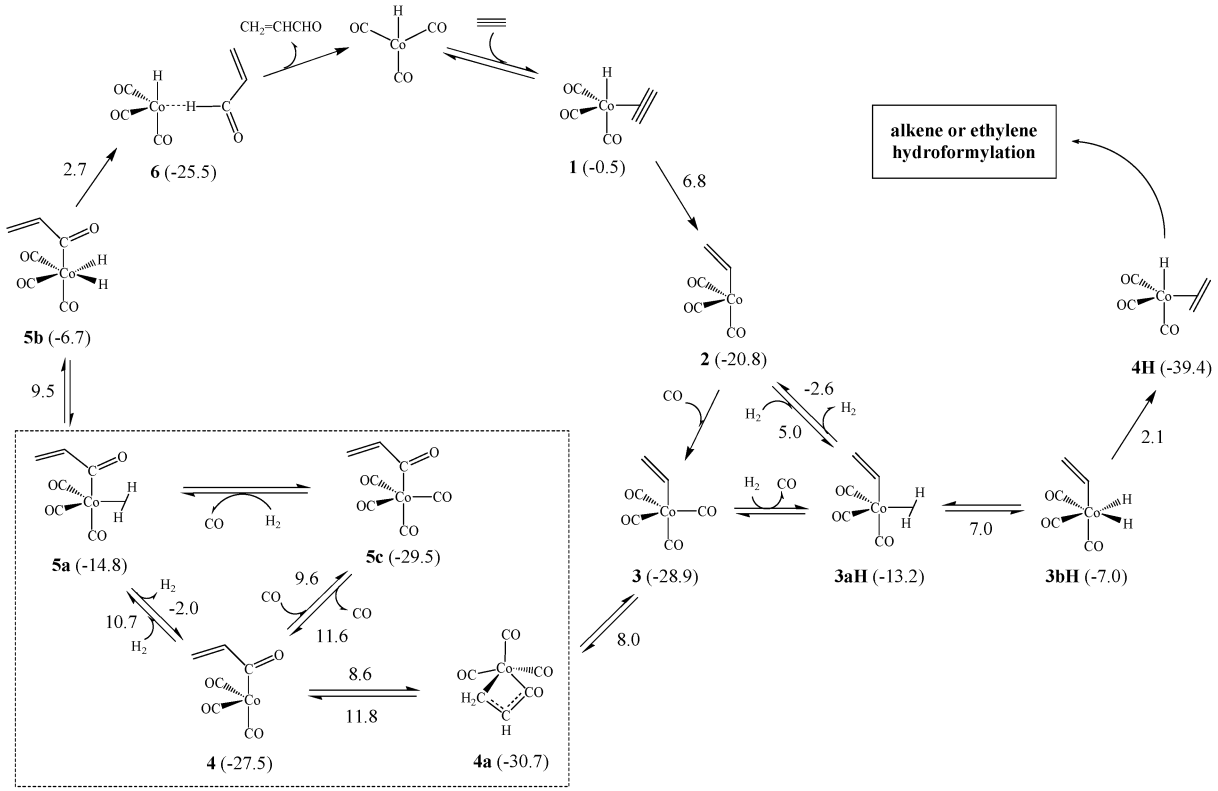

former process is more exergonic than the latter by 13.9 kcal/mol. This thermodynamic difference provides an opportunity for the optimization or manipulation of reaction conditions for the desired rate and/or products.

The successive carbonylation of $(H_2C{=}CH)Co(CO)_4$ (**3**) occurs in two steps. First, the vinyl group migrates to a cis carbonyl coupled with a skeletal change leading to the most stable acyl complex, $(\eta^3\text{-}H_2C{=}CHCO)Co(CO)_3$ (**4a**). Second, **4a** transforms to the less stable complex $(\eta^2\text{-}O{=}CCHCH_2)Co(CO)_3$ (**4**) with the acyl group at the axial position and additional η^2-O=C stabilization.

Furthermore, the H_2 oxidative addition occurs on the η^2-acyl complex **4**, while the alternative case of H_2 addition to η^3-acyl complex **4a** is ruled out from the kinetic point of view. The H_2 coordination and oxidative addition to the η^2-O=C acyl complex are computed to be endergonic processes (12.7 and 8.1 kcal/mol). The competitive side reaction is the CO coordination for the formation of $(H_2C{=}CHCO)Co(CO)_4$ (**5c**), which is exergonic by 2.0 kcal/mol. Thus, the formation of **5c** is more favored thermodynamically and is also dominant in the possible equilibrium between $(H_2C{=}CHCO)Co(CO)_4$ (**5c**) and $(H_2C{=}CHCO)Co(CO)_3(\eta^2\text{-}H_2)$ (**5a**), as shown in eq 1. Next, the elimination of acrolein from complex **5b** goes via a three-centered transition state leading to the adduct **6**, in which acrolein coordinates with $HCo(CO)_3$ through the aldehyde hydrogen atom.

On the basis of the constructed catalytic cycle in Scheme 2, it is very interesting to determine the rate-determining step of the entire reaction. For example, the isomerization from **4a** to **4** and the CO dissociation from **5c** to **4** as well as H_2 coordination from **4** to **5a** have very close activation free energies (10.7−11.8 kcal/mol). Therefore, each of them around **4** (in a dotted box) can be the rate-determining step with variation in the reaction conditions (temperature, pressure, and solvent).

Acknowledgment. This work was supported by the Chinese Academy of Sciences (Grant No. 20029908) and the National Natural Science Foundation of China.

Supporting Information Available: Tables giving total electronic energies and zero-point energies (ZPE) as well as thermal corrections to enthalpies and thermal corrections to Gibbs free energies (403.15 K, 200 atm) for all systems and Cartesian coordinates for each species presented in the catalytic cycle. This material is available free of charge via the Internet at http://pubs.acs.org.

OM034212R